

LOCI OF 3-PERIODICS IN AN ELLIPTIC BILLIARD: WHY SO MANY ELLIPSES?

RONALDO GARCIA, DAN REZNIK, AND JAIR KOILLER

ABSTRACT. We analyze the family of 3-periodic (triangular) trajectories in an Elliptic Billiard. Specifically, the loci of their Triangle Centers such as the Incenter, Barycenter, etc. Many points have ellipses as loci, but some are also quartics, self-intersecting curves of higher degree, and even a stationary point. Elegant proofs have surfaced for locus ellipticity of a few classic centers, however these are based on laborious case-by-case analysis. Here we present two rigorous methods to detect when any given Center produces an elliptic locus: a first one which is a hybrid of numeric and computer algebra techniques (good for fast detection only), and a second one based on the Theory of Resultants, which computes the implicit two-variable polynomial whose zero set contains the locus.

Keywords: elliptic billiard, periodic trajectories, triangle center, derived triangle, locus, loci, algebraic.

MSC2010 37-40 and 51N20 and 51M04 and 51-04

1. INTRODUCTION

We’ve been interested in properties and invariants of the family of 3-periodics (orbits) in an Elliptic Billiard (EB), see Appendix A for a review. This triangle family exhibits remarkable invariants¹ including: (i) the ratio of Inradius-to-Circumradius (equivalent to constant sum of orbit cosines), (ii) all triangles share a common *Mittenpunkt*², located at the EB center, and (iii) a well-known derived circle³ is stationary [19]. Surprisingly, certain invariants generalize to N -periodics, $N > 3$ [1, 2, 19].

Here we focus on a related set of phenomena: the loci of *Triangle Centers* [11] such as the Incenter, Barycenter, etc., over the family of 3-periodic orbits. We adopt Kimberling’s nomenclature X_i [12], e.g., X_1 for the Incenter, X_2 for the Barycenter, X_3 for the Circumcenter, etc. Triangle Centers are reviewed in and constructions for a few basic ones appear in Appendix B.

¹See videos on Table 5 in Section 5.

²Where lines drawn from the Excenters through sides’ midpoints meet [28].

³The *Cosine Circle* [28] of the Excentral Triangle has constant radius and is concentric with the EB [19].

An early experimental result was that the locus of the Incenter X_1 was an ellipse though that of the Intouchpoints⁴ was a self-intersecting curve, Figure 1 (left).

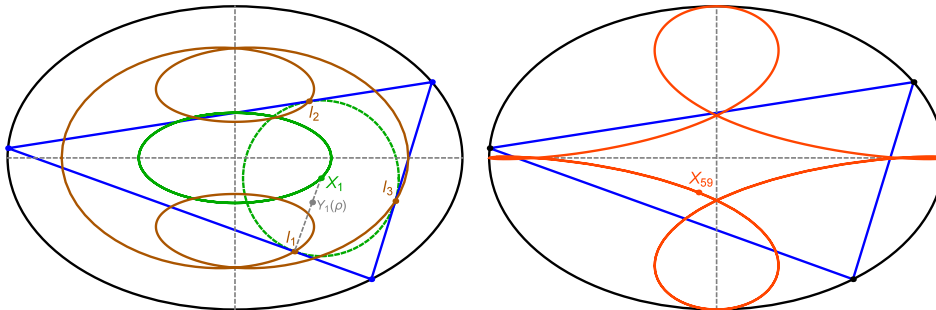


FIGURE 1. **Left:** An EB (black), a sample orbit (blue), the elliptic locus of the Incenter X_1 (green) and of that of the Intouchpoints I_1, I_2, I_3 (brown), the points of contact of the Incircle (dashed green) with the orbit sides. These produce a curve with two internal lobes whose degree is at least 6. $Y_1(\rho)$ is a convex combination of X_1 and I_1 referred to in Section 3.5. **Video:** [18, pl#01,02]. **Right:** The locus of X_{59} is a curve with four self-intersections. A vertical line epsilon away from the origin intersects the locus at 6 points.

The former observation was quite unexpected for two reasons: the explicit expressions for 3-periodic vertices are complicated and highly non-linear, see Appendix C. Secondly, obtaining the Incenter from these requires a second non-linear transformation. We were pleased when this fact was elegantly proven via Complexification [21]. Proofs soon followed for the ellipticity of both X_2 [14] and X_3 [5, 7], drawing upon Algebraic and/or Analytic Geometry. However, each takes Triangle Centers on a case-by-case basis. How could one scale such proofs to a longer list of centers, e.g., the thousands catalogued in [12]?

Take for example, the case of the locus of X_{59} , Figure 1(right). Its locus is clearly non-elliptic, with 4 self-intersections. What is the nature of this phenomenon?

Consider also that a few loci look nearly elliptic but aren't, see our locus gallery in [17]. An emblematic case is that of X_6 , the Symmedian Point⁵, explored in Section 3.4: numerically we could tell its locus was not elliptic⁶ but to the naked eye it looked perfectly so.

All of the above indicates a proper theory for locus curve type is in order. We are far from this goal, though our results present two compromises.

⁴Where the Incircle touches a triangle's sides [28].

⁵Where *Symmedians* meet – lines drawn from vertices to opposite sides' midpoints, reflected about angular bisectors [28, Symmedian Point].

⁶Below we show it to be a convex quartic.

1.1. Results. We present a method to rigorously verify when any Triangle Center, regardless of its construction, has an elliptic locus. We apply this method to the first 100 Centers listed in [12], finding that a full 29 are elliptic. Explicit expressions for their axes are provided in Appendix E. We also show that when said centers are rational functions on the sidelengths, loci (elliptic or not) will be algebraic curves. We also describe a method based on the theory of resultants which computes the irreducible polynomial in two variables, whose zero set is the Zariski Closure [3] of the locus.

1.2. Outline. We start reviewing previous results, Section 2. Main results appear in Sections 3 and 4. In the former we describe our new proof method and in the latter we present our resultants-base elimination method to compute the Zariski closure of rational Centers. We conclude in Section 5 with a list of questions and interesting links and videos. The Appendices review foundations and are also where longer calculations and tables appear.

2. EARLIER OBSERVATIONS

Kimberling’s Encyclopedia of Triangle Centers (ETC) [12] describes constructions and properties for thousands⁷ such Centers, identified as X_i : X_1 for Incenter, X_2 for Barycenter, etc. Trilinear and/or Barycentric Coordinates are also provided for each Center, see Appendix B for details. The former are signed distances to the sides of a triangle $T = P_1P_2P_3$, i.e. they are invariant with respect to similarity/reflection transformations, see Figure 2.

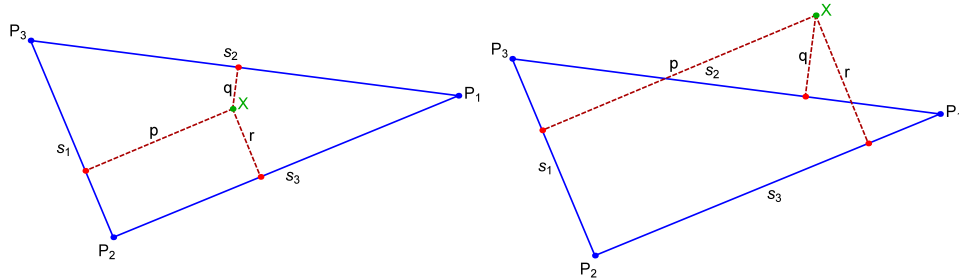


FIGURE 2. Trilinear coordinates $p : q : r$ for a point X on the plane of a generic triangle $T = P_1P_2P_3$ are homogeneous signed distances to each side whose lengths are s_1, s_2, s_3 . The red dots are known as the *pedal points* of X [28]. The left (resp. right) figure shows an interior (resp. exterior) point. In both cases p, r are positive however q is positive (resp. negative) in the former (resp. latter) case.

Trilinears can be easily converted to Cartesians using [28]:

$$(1) \quad X = \frac{ps_1P_1 + qs_2P_2 + rs_3P_3}{ps_1 + qs_2 + rs_3}$$

⁷Kimberling logs 37 thousand at the time of this writing!

where $s_1 = |P_3 - P_2|$, $s_2 = |P_1 - P_3|$ and $s_3 = |P_2 - P_1|$ are the sidelengths, Figure 2. For instance, the Trilinears for the barycenter are $p = s_1^{-1}$, $q = s_2^{-1}$, $r = s_3^{-1}$, yielding the familiar $X_2 = (P_1 + P_2 + P_3)/3$.

We show that the locus of exactly 29 out of the first 100 Kimberling Centers are ellipses. Figure 3 (left) illustrates the first five Kimberling Centers, all elliptic, with X_4 , X_5 shown there being new results.

We have also observed that the locus of the Feuerbach Point X_{11} coincides with the $N = 3$ *Caustic*, a confocal ellipse to which the 3-periodic family is internally tangent, Appendix A. Additionally, the locus of X_{100} , the Anticomplement⁸ of X_{11} is the EB boundary! These phenomena appear in Figure 3 (right).

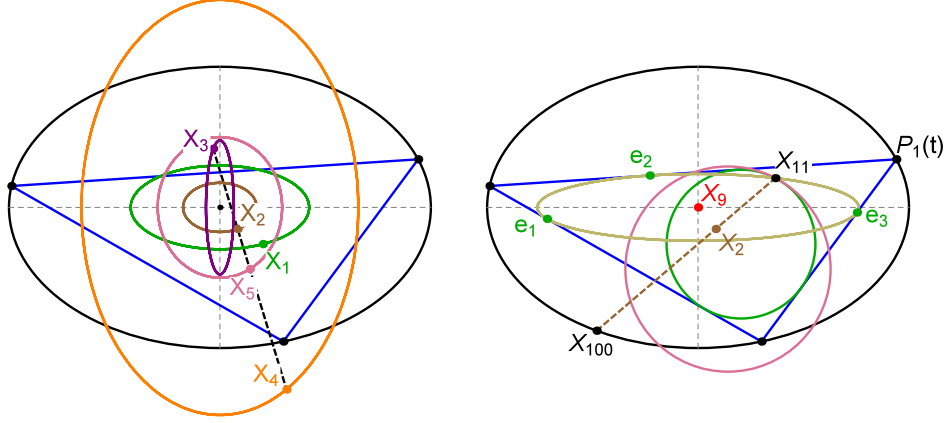


FIGURE 3. **Left:** The loci of Incenter X_1 , Barycenter X_2 , Circumcenter X_3 , Orthocenter X_4 , and Center of the 9-Point Circle X_5 are all ellipses, [Video](#) [18, pl#05]. Also shown is the *Euler Line* (dashed black) which for any triangle, passes through all of X_i , $i = 1...5$ [28]. **Right:** A 3-periodic orbit starting at $P_1(t)$ is shown (blue). The locus of X_{11} , where the Incircle (green) and 9-Point Circle (pink) meet, is the *Caustic* (brown), also swept by the Extouchpoints e_i . X_{100} (double-length reflection of X_{11} about X_2) is the EB. **Video:** [18, pl#07]. Reproduced from [19].

⁸Double-length reflection about the Centroid X_2 .

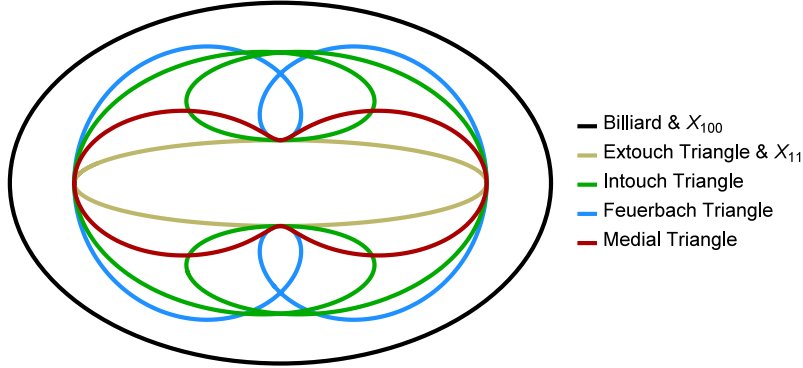


FIGURE 4. Loci generated by the vertices of selected orbit-Derived Triangles, namely: the Intouch (green), Feuerbach^a (blue), and Medial (red) Triangles are non-elliptic. However, those of the Extouch Triangle (brown), are identical to the $N = 3$ Caustic (a curve also swept by X_{11}). Not shown is the locus of the Excentral Triangle, an ellipse similar to a rotated copy of the Incenter locus. **Video:** [18, pl#02,06,07,09]

^aNot to be confused with the Feuerbach Point X_{11} . The Feuerbach Triangle has vertices at the three contact points of the 9-point Circle with the Excircles [28].

Additionally, a few observations have been made [19] about the loci of vertices orbit-derived triangles (see Appendix B.2), some of which are elliptic and others non, illustrated in Figure 4.

A related result co-discovered by Peter Moses [12, X(9)] and Deko Dekov [9] is that 57 Triangle Centers lie on what they call the “Mittenpunkt-centered Circumellipse”. This is equivalent to stating that the loci of all such points is the EB boundary, since the 3-periodic family has a stationary Mittenpunkt [19]. An animation of some of Peter Moses’ points is viewable in [18, pl#10].

3. DETECTING ELLIPTIC LOCI

Let the boundary of the EB be given by $(a > b > 0)$:

$$(2) \quad f(x, y) = \left(\frac{x}{a}\right)^2 + \left(\frac{y}{b}\right)^2 = 1.$$

We describe a numerically-assisted method⁹ which proves that the locus of a given Triangular Center is elliptic or otherwise. We then apply it to the first 100 Triangle Centers¹⁰ listed in [12].

3.1. Proof Method. Our proof method consists of two phases, one numeric, and one symbolic, Figure 6. It makes use of the following Lemmas, whose proofs appear in Appendix D:

Lemma 1. *The locus of a Triangle Center X_i is symmetric about both EB axes and centered on the latter’s origin.*

⁹We started with visual inspection, but this is both laborious and unreliable, some loci (take X_{30} and X_6 as examples) are indistinguishable from ellipses to the naked eye.

¹⁰An arbitrarily large list can be tested.

Proof. Given a 3-periodic $T = P_1P_2P_3$. Since the EB is symmetric about its axes, the family will contain the reflection of T about said axes, call these T' and T'' . Since Triangle Centers are invariant with respect to reflections, Appendix B, X'_i and X''_i will be found at similar reflected locations. \square

Lemma 2. *Any Triangle Center X_i of an isosceles triangle is on the axis of symmetry of said triangle.*

Lemma 3. *If the locus of Triangle Center X_i is elliptic, said ellipse must be concentric and axis-aligned with the EB.*

Lemma 4. *A parametric traversal of P_1 around the EB boundary triple covers the locus of Triangle Center X_i , elliptic or not.*

See Section 3.5 for more details.

A first phase fits a concentric, axis-aligned ellipse to a fine sampling of the locus of some Triangle Center X_i . A good fit occurs when the error is several orders of magnitude¹¹ less than the sum of axes regressed by the process. False negatives are eliminated by setting the error threshold to numeric precision. False positives can be produced by adding arbitrarily small noise to samples of a perfect ellipse, though this type of misclassification does not survive the next, symbolic phase.

A second phase attempts to symbolically verify via a Computer Algebra System (CAS) if the parametric locus of the X_i satisfies the equation of a concentric, axis-aligned ellipse. Expressions for its semi-axes are obtained by evaluating X_i at isosceles orbit configurations, Figure 5. The method is explained in detail in Figure 7.

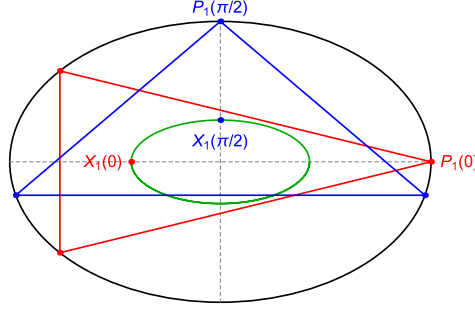


FIGURE 5. With P_1 at the right (resp. top) vertex of the EB, the orbit is a sideways (resp. upright) isosceles triangle, solid red (resp. solid blue). Not shown are their two symmetric reflections. Also shown (green) is the locus of a sample Triangle Center, X_1 in this case. At the isosceles positions, vertices will lie on the axis of symmetry of the triangle, Lemma 2. When the locus is elliptic, the x, y coordinates of $X_i(0), X_i(\pi/2)$ are the semi-axes a_i, b_i , respectively.

¹¹Robust fitting of ellipses to a cloud of points is not new [6]. In our case, the only source of error in Triangle Center coordinates is numerical precision, whose propagation can be bounded by Interval Analysis [15, 24].

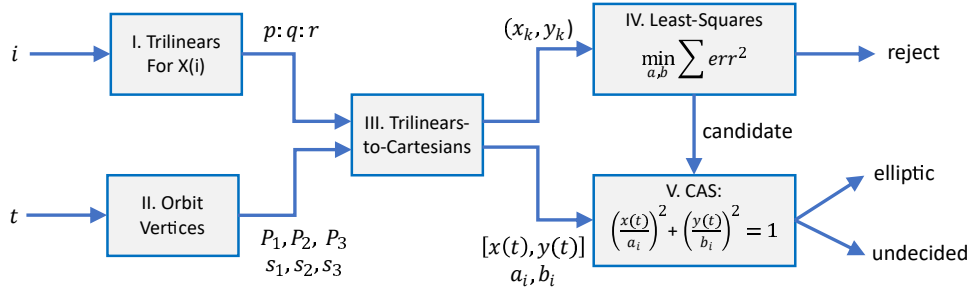


FIGURE 6. Our method as a flow-chart, modules labeled from I to V: (I) The i th center is specified and its Trilinears $p : q : r$ are obtained from ETC [12]. (II) Given a symbolic parameter t or a numeric sample t_k , obtain Cartesians for orbit vertices, Appendix C.2. (III) Combine Trilinears and orbit data to obtain, via (1), numeric Cartesians for $X_i(t_k)$ or symbolically as $X_i(t)$. (IV) Least-squares fit an axis-aligned, concentric ellipse to the (x_k, y_k) samples and accept X_i as candidate if the fit error is sufficiently small. (V) Verify, via a Computer Algebra System (CAS), if the parametric locus $X_i(t)$ satisfies the equation of an ellipse whose axes a_i, b_i are obtained symbolically in II-III by setting $t = 0, \pi/2$. If the CAS is successful, $X_i(t)$ is deemed elliptic, otherwise the result is “undecided”. The CAS was successful for all 29 candidates selected by IV out of the first 100 Kimberling Centers.

1. Select Candidates:

- Let the EB have axes a, b such that $a > b > 0$. Calculate $P_1(t_k) = (a \cos(t_k), b \sin(t_k))$, for M equally-spaced samples $t_k \in [0, 2\pi)$, $k = 1, 2, \dots, M$.
- Obtain the Cartesian coordinates for the orbit vertices $P_2(t_k)$ and $P_3(t_k)$, $\forall k$ (Appendix C.2).
- Obtain the Cartesians for Triangle Center X_i from its Trilinears (1), for $\forall t_k$. If analyzing the vertex of a Derived Triangle, convert a row of its *Trilinear Matrix* to Cartesians, Appendix B.2.
- Least-squares fit an origin-centered, axis-aligned ellipse (2 parameters) to the $X_i(t_k)$ samples, Lemma 3. Accept the locus as potentially elliptic if the numeric fit error is negligible, rejecting it otherwise.

2. Verify with CAS

- Taking a, b as symbolic variables, calculate $X_i(0)$ (resp. $X_i(\pi/2)$), placing P_1 at the right (resp. top) EB vertex. The orbit will be a sideways (resp. upright) isosceles triangle, Figure 5. By Lemma 2, X_i will fall along the axis of symmetry of either isosceles.
- The x coordinate of $X_i(0)$ (resp. the y of $X_i(\pi/2)$) will be symbolic expressions in a, b . Use them as candidate locus semiaxes’ lengths a_i, b_i .
- Taking t as a symbolic variable, use a computer algebra system (CAS) to verify if $X_i(t) = (x_i(t), y_i(t))$, as parametrics on t , satisfy $(x_i(t)/a_i)^2 + (y_i(t)/b_i)^2 = 1$, $\forall t$.
- If the CAS is successful, Lemma 4 guarantees $X_i(t)$ will cover the entire ellipse, so assert that the locus of X_i is an ellipse. Else, locus ellipticity is indeterminate.

FIGURE 7. Method for detecting ellipticity of a Triangle Center locus.

3.2. Phase 1: Least-Squares-Based Candidate Selection. Let the position of $X_i(t)$ be sampled¹² at $t_k \in [0, 2\pi]$, $k = 1 \dots M$. If the locus is an ellipse, then the latter is concentric and axis-aligned with the EB, Lemma 3. Express the squared error as the sum of squared sample deviations from an implicit ellipse:

$$(3) \quad \text{err}^2(a_i, b_i) = \sum_{k=1}^M \left[\left(\frac{x_k}{a_i} \right)^2 + \left(\frac{y_k}{b_i} \right)^2 - 1 \right]^2$$

Least-squares can be used to estimate the semi-axes:

$$(\hat{a}_i, \hat{b}_i) = \arg \min_{a, b} \{ \text{err}^2(a_i, b_i) \}$$

The first 100 Kimberling centers separate into two distinct clusters: 29 with negligible least-squares error, and 71 with finite ones. These are shown in ascending order of error in Figure 8. For reference, Appendix F provides errors for $a/b = 1.5$ in tabular form.

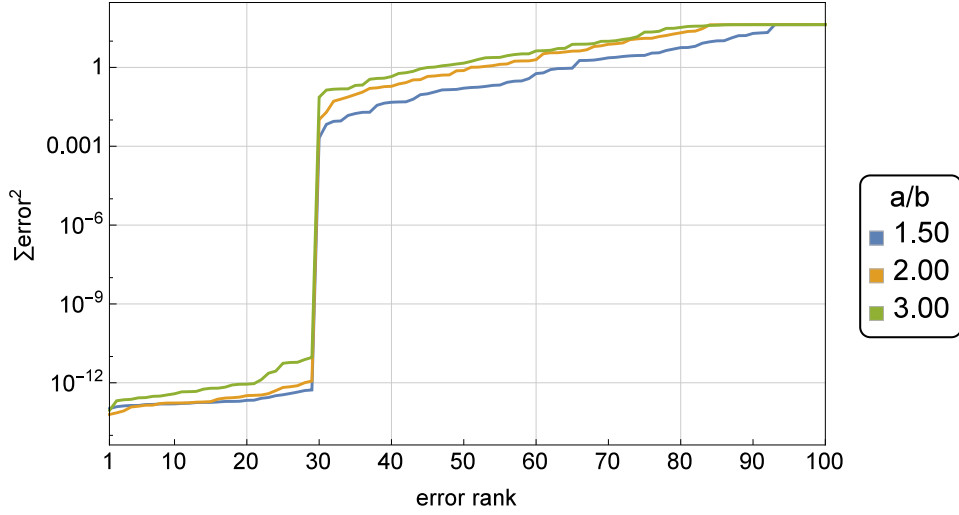


FIGURE 8. Log of Least-squares error for first 100 Kimberling centers in ascending order of error, for three values of a/b , $M = 1500$. Elliptic vs. non-elliptic centers are clearly separated in two groups whose errors differ by several orders of magnitude. Table 6, Appendix F shows that X_{37} and X_6 are have ranks 30 and 31 respectively, i.e., they are the Centers whose non-elliptic loci are closest to a perfect ellipse.

A gallery of loci generated by X_1 to X_{100} (as well as vertices of several derived triangles) is provided in [17].

¹²Randomly or in equal intervals.

3.3. Phase 2: Symbolic Verification with a CAS. A CAS was successful in symbolically verifying that all 29 candidates selected in Phase 1 satisfy the equation of an ellipse (none were undecided). As an intermediate step, explicit expressions for their elliptic semi-axes were computed, listed in Appendix E.

Theorem 1. *Out of the first 100 centers in [12], exactly 29 produce elliptic loci, all of which are concentric and axis-aligned with the EB. These are $X_{i,i=1, 2, 3, 4, 5, 7, 8, 10, 11, 12, 20, 21, 35, 36, 40, 46, 55, 57, 63, 65, 72, 78, 79, 80, 84, 88, 90}$. Specifically:*

- *The loci of $X_i, i = 2, 7, 57, 63$ are ellipses similar to the EB.*
- *The loci of $X_i, i = 4, 10, 40$ are ellipses similar to a 90° -rotated copy of the EB.*
- *The loci of $X_i, i = 88, 100$ are ellipses identical to the EB¹³.*
- *The loci of X_{55} is an ellipse similar to the $N = 3$ Caustic.*
- *The loci of $X_i, i = 3, 84$ are ellipses similar to a 90° -rotated copy of the $N = 3$ Caustic.*
- *The locus of X_{11} is an ellipse identical to the $N = 3$ Caustic.*

The properties above are summarized on Table 1. Explicit expressions for the semi-axes in terms of a, b for the above appear in Appendix E.

row	X_i	definition	sim	row	X_i	definition	sim
1	1	Incenter	J^t	16	46	X_4 -Ceva Conj. of X_1	
2	2	Centroid	B	17	55	Insimilictr(Circumc., Incir.)	C
3	3	Circumcenter	C^t	18	56	Exsimilictr(Circumc., Incir.)	
4	4	Orthocenter	B^t	19	57	Isogonal Conj. of X_9	B
5	5	9-Point Center		20	63	Isogonal Conj. of X_{19}	B
6	7	Gergonne Point	B	21	65	Intouch Triangle's X_4	
7	8	Nagel Point		22	72	Isogonal Conj. of X_{28}	J
8	10	Spieker Center	B^t	23	78	Isogonal Conj. of X_{34}	
9	11	Feuerbach Point	C^+	24	79	Isogonal Conj. of X_{35}	
10	12	$\{X_{1,5}\}$ -Harm.Conj. of X_{11}		25	80	Refl. of X_1 about X_{11}	J^t
11	20	de Longchamps Point		26	84	Isogonal Conj. of X_{40}	C^t
12	21	Schiffler Point		27	88	Isogonal Conj. of X_{44}	B^+
13	35	$\{X_{1,3}\}$ -Harm.Conj. of X_{36}		28	90	X_3 -Cross Conj. of X_1	
14	36	Inverse-in-Circumc. of X_1		29	100	Anticomplement of X_{11}	B^+
15	40	Bevan Point	B^t				

TABLE 1. The 29 Kimberling centers within X_1 to X_{100} with elliptic loci. Under column “sim.”, letters B,C,J indicate the locus is similar to EB, Caustic, or Excentral locus, respectively. An additional + (resp. t) exponent indicates the locus is identical (resp. similar to a perpendicular copy) to the indicated ellipse. Note: the ellipticity of $X_{i,i = 1, 2, 3, 4}$ was previously proven [21, 27, 5, 7].

3.4. The quartic locus of the Symmedian Point. At $a/b = 1.5$ the locus of X_6 , the Symmedian Point, is visually indistinguishable from an

¹³See below for more centers on the EB discovered by Peter Moses and Deko Dekov.

ellipse, Figure 9. Fortunately, its fit error is 10 orders of magnitude higher than the ones produced by true elliptic loci, see Table 6 in Appendix F. So it is easily rejected by the least-squares phase. Indeed, symbolic manipulation yields:

Theorem 2. *The locus of X_6 is a convex quartic given by:*

$$\mathcal{X}_6(x, y) = c_1x^4 + c_2y^4 + c_3x^2y^2 + c_4x^2 + c_5y^2 = 0$$

where:

$$\begin{aligned} c_1 &= b^4(5\delta^2 - 4(a^2 - b^2)\delta - a^2b^2) & c_2 &= a^4(5\delta^2 + 4(a^2 - b^2)\delta - a^2b^2) \\ c_3 &= 2a^2b^2(a^2b^2 + 3\delta^2) & c_4 &= a^2b^4(3b^4 + 2(2a^2 - b^2)\delta - 5\delta^2) \\ c_5 &= a^4b^2(3a^4 + 2(2b^2 - a^2)\delta - 5\delta^2) & \delta &= \sqrt{a^4 - a^2b^2 + b^4} \end{aligned}$$

Proof. Using a CAS, obtain symbolic expressions for the coefficients of a quartic symmetric about both axes (no odd-degree terms), passing through 5 known-points. Still using a CAS, verify the symbolic parametric for the locus satisfies the quartic. \square

Note the above is also satisfied by a degenerate level curve $(x, y) = 0$, which we ignore.

Remark 1. *The axis-aligned ellipse \mathcal{E}_6 with semi-axes a_6, b_6 is internally tangent to $\mathcal{X}_6(x, y) = 0$ at the four vertices where:*

$$(4) \quad a_6 = \frac{[(3a^2 - b^2)\delta - (a^2 + b^2)b^2]a}{a^2b^2 + 3\delta^2}, \quad b_6 = \frac{[(a^2 - 3b^2)\delta + (a^2 + b^2)a^2]b}{a^2b^2 + 3\delta^2}$$

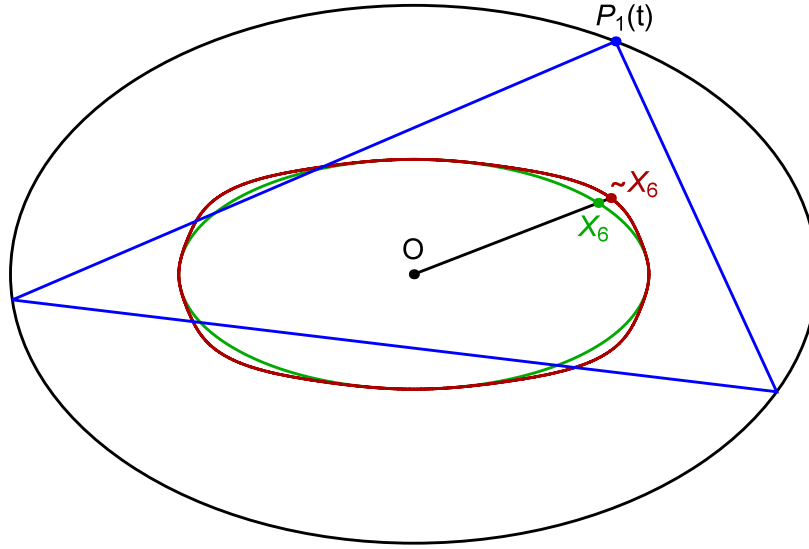


FIGURE 9. An $a/b = 1.5$ EB is shown (black) as well as a sample 3-periodic (blue). At this aspect ratio, the locus of X_6 (green) is indistinguishable to the naked eye from a perfect ellipse. To see it is non-elliptic, consider the locus of a point $\sim X_6(t) = X_6(t) + k|X_6(t) - Y'_6(t)|$, with $k = 2 \times 10^6$ and $Y'_6(t)$ the intersection of $OX_6(t)$ with a best-fit ellipse (visually indistinguishable from green), (4).

Table 2 shows the above coefficients numerically for a few values of a/b .

a/b	a_6	b_6	c_1/c_3	c_2/c_3	c_4/c_3	c_5/c_3	$A(\mathcal{E}_6)/A(\mathcal{X}_6)$
1.25	0.433	0.282	0.211	1.185	-0.040	-0.095	0.9999
1.50	0.874	0.427	0.114	2.184	-0.087	-0.399	0.9998
2.00	1.612	0.549	0.052	4.850	-0.134	-1.461	0.9983
3.00	2.791	0.620	0.020	12.423	-0.157	-4.769	0.9949

TABLE 2. Coefficients c_i/c_3 , $i = 1, 2, 4, 5$ for the quartic locus of X_6 as well as the axes a_6, b_6 for the best-fit ellipse, for various values of a/b . The last-column reports the area ratio of the internal ellipse \mathcal{E}_6 (with axes a_6, b_6) to that of the quartic locus \mathcal{X}_6 , showing an almost exact match.

3.5. Locus Triple Winding. As an illustration to Lemma 4, consider the elliptic locus of X_1 , the Incenter¹⁴. Consider the locus of a point Y_1 located on between X_1 and an Intouchpoint I_1 , Figure 1 (left):

$$Y_1(t; \rho) = (1 - \rho)X_1(t) + \rho I_1(t), \quad \rho \in [0, 1]$$

When $\rho = 1$ (resp. 0), $Y_1(t)$ is the two-lobe locus of the Intouchpoints (resp. the elliptic locus of X_1). With ρ just above zero, Y_1 winds thrice around the

¹⁴The same argument is valid for the non-elliptic locus of, e.g., X_{59} , Figure 1 (right).

EB center. At $\rho = 0$, the two lobes and the remainder of the locus become one and the same: Y_1 winds thrice over the locus of the Incenter, i.e., the latter is the limit of such a convex combination.

It can be shown that at $\rho = \rho^*$, with $\rho^* = 1 - (b/a)^2$, the two $Y_1(t)$ lobes touch at the the EB center. When $\rho > \rho^*$ (resp. $\rho < \rho^*$), the locus of $Y_1(t)$ has winding number 1 (resp. 3) with respect to the EB center, see Figure 10.

A similar phenomenon occurs for loci of convex combinations of the following pairs: (i) Barycenter X_2 and a side midpoint, (ii) Circumcenter X_3 and a side midpoint, (iii) Orthocenter X_4 and altitude foot, etc., see [18, pl#11,12].

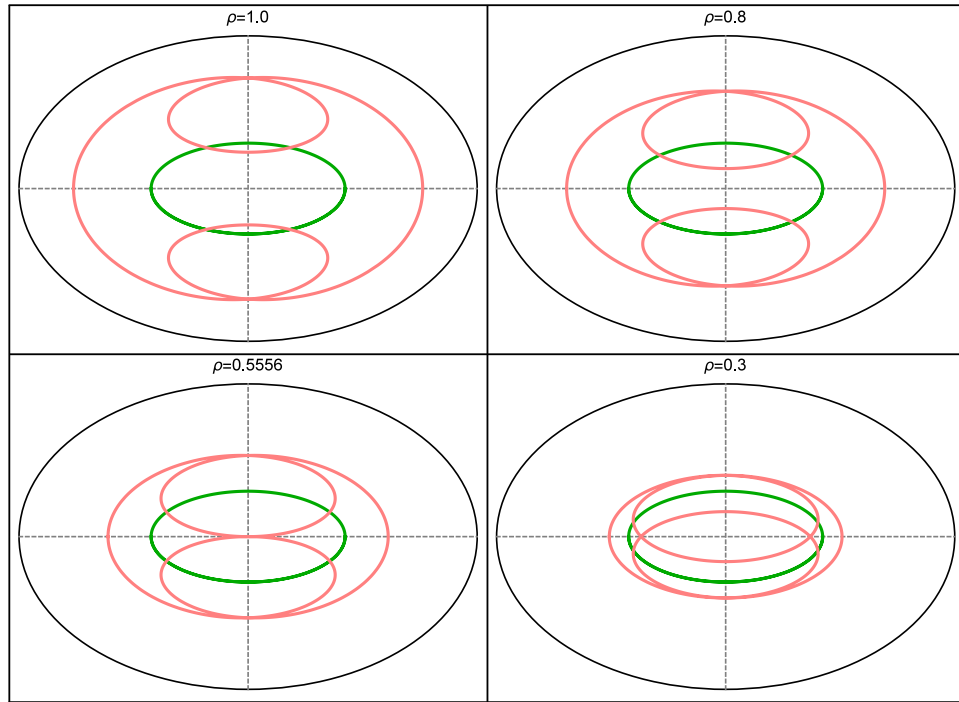


FIGURE 10. An $a/b = 1.5$ EB is shown (black) as well as the elliptic locus of X_1 (green) and the locus of $Y_1(t)$ (pink), the convex combination of $X_1(t)$ and an Intouchpoint given by a parameter $\rho \in [0, 1]$, see Figure 1(left). At $\rho = 1$ (top-left), $Y_1(t)$ is the two-lobe locus of the Intouchpoint. For every tour of an orbit vertex $P_1(t)$ around the EB, $Y_1(t)$ winds once over its locus. At $\rho = 0.8$ (top-right) the lobes approach each other but still lie in different half planes. At $\rho = \rho^* = 1 - (b/a)^2$, the lobes touch at the EB center (bottom-left). If $\rho \in (0, \rho^*)$, the two lobes self-intersect twice. As $\rho \rightarrow 0$, the two lobes become nearly coincidental (bottom-right). At $\rho = 0$, the Y_1 locus with its two lobes all collapse to the Incenter locus ellipse (green), in such a way that for every tour of $P_1(t)$ around the EB, X_1 winds thrice over its locus. **Video:** [18, pl#11,12]

4. TOWARD A TYPIFICATION OF LOCI

In this section we take initial steps toward relating Trilinears to a locus curve type. Our goal is to set up a Computational Algebraic Geometry context useful for practitioners.

4.1. Trilinears: No Apparent Pattern. When one looks at a few examples of Triangle Centers whose loci are elliptic vs non, one finds no apparent algebraic pattern in said Trilinears, Table 3.

center	name	$h(s_1, s_2, s_3)$
X_1	Incenter	1
X_2	Centroid	$1/s_1$
X_3	Circumcenter	$s_1(s_2^2 + s_3^2 - s_1^2)$
X_4	Orthocenter	$1/[s_1(s_2^2 + s_3^2 - s_1^2)]$
X_5	9-Point Center	$s_2 s_3 [s_1^2(s_2^2 + s_3^2) - (s_2^2 - s_3^2)^2]$
X_{11}	Feuerbach Point	$s_2 s_3 (s_2 + s_3 - s_1)(s_2 - s_3)^2$
X_{88}	Isog. Conjug. of X_{44}	$1/(s_2 + s_3 - 2s_1)$
X_{100}	Anticomplement of X_{11}	$1/(s_2 - s_3)$
X_6	Symmedian Point	s_1
X_{13}^*	Fermat Point	$s_1^4 - 2(s_2^2 - s_3^2)^2 + s_1^2(s_2^2 + s_3^2 + 4\sqrt{3}A)$
X_{15}^*	2nd Isodynamic Point	$s_1[\sqrt{3}(s_1^2 - s_2^2 - s_3^2) - 4A]$
X_{19}	Clawson Point	$1/(s_2^2 + s_3^2 - s_1^2)$
X_{37}	Crosspoint of X_1, X_2	$s_2 + s_3$
X_{59}	Isog. Conj. of X_{11}	$1/[s_2 s_3 (s_2 + s_3 - s_1)(s_2 - s_3)^2]$
X_9	Mittenpunkt	$s_2 + s_3 - s_1$

TABLE 3. Triangle Center Function h for a few selected X_i 's, taken from [12]. The first 8 centers produce elliptic loci, whereas the remainder (**boldfaced**) do not. X_{13} and X_{15} are *starred* to indicate their Trilinears are irrational: these contain A , the area the triangle, known (e.g., from Heron's formula) to be irrational on the sidelengths. We haven't yet detected an algebraic pattern which differentiates both groups, nor have we detected an irrational Center whose locus is elliptic. Regarding the last row, the Mittenpunkt, we don't consider its locus to be elliptic since it degenerates to a point at the EB center.

A few observations include:

- The locus of a Triangle Center is symmetric about both EB axes, Lemma 1, Appendix 4.
- There are Trilinears Centers rational on the sidelengths which produce (i) elliptic loci (e.g., X_1, X_2 , etc.) as well as (ii) non-elliptic (e.g., X_6, X_{19} , etc.).
- No locus has been found with more than 6 intersections with a straight line, suggesting the degree is at most 6.
- No Center has been found with irrational Trilinears whose locus is an ellipse¹⁵, suggesting that the locus of irrational Centers is always non-elliptic.

4.2. An Algebro-Geometric Ambient. Given EB semi-axes a, b , our problem can be described by the following 14 variables:

- 6 triangle vertex coordinates, $P_i = (x_i, y_i)$, $i = 1, 2, 3$;
- 3 sidelengths s_1, s_2, s_3 ;
- 3 Trilinears p, q, r ;

¹⁵Not shown, but also tested were irrational Triangle Centers X_j , $j = 14, 16, 17, 18, 359, 360, 364, 365, 367$.

- 2 locus coordinates x, y .

These are related by the following system of 14 polynomial equations:

eqns.	description	zero set of
3	vertices on the EB	$(x_i/a)^2 + (y_i/b)^2 - 1, i = 1, 2, 3$
3	reflection law at P_j j, k, ℓ cyclic, $\mathcal{A} = \text{diag}(1/a^2; 1/b^2)$	$(AP_j.P_\ell - AP_j.P_j)(P_k - P_j)^2$ $-(AP_j.P_k - AP_j.P_j)(P_\ell - P_j)^2$
3	sidelengths	$(x_i - x_j)^2 + (y_i - y_j)^2 - s_k^2$
2	locus Cartesians, (1)	$(ps_1 + qs_2 + rs_3)(x, y) - ps_1P_1 + qs_2P_2 + rs_3P_3$
3	trilinears (must rationalize)	$p - h(s_1, s_2, s_3); q - h(s_2, s_3, s_1); r - h(s_3, s_1, s_2)$

Billiard Integrability (Appendix A) implies that out of the first 6 equations, one is functionally dependent on the rest. Therefore, we have 13 independent equations in 14 variables, yielding a 1d algebraic variety, which can be complexified if desired.

Can tools from computational Algebraic Geometry [23, 25] be used to eliminate 12 variables automatically, thus obtaining a single polynomial equation $\mathcal{L}(x, y) = 0$ whose Zariski closure contains the locus? Below we provide a method based on the theory of resultants [13, 25] to compute \mathcal{L} for a subset of Triangle Centers.

4.3. When Trilinears are Rational. Consider a Triangle Center X whose Trilinears $p : q : r$ are rational on the sidelengths s_1, s_2, s_3 , i.e., the Triangle Center Function h is rational, (5). We provide a 3-step method to compute the algebraic curve $\mathcal{L}(x, y) = 0$. We refer to Lemmas 5 and 6 appearing below. Appendix C contains supporting expressions.

Step 1. *Introduce the symbolic variables u, u_1, u_2 :*

$$u^2 + u_1^2 = 1, \quad \rho_1 u^2 + u_2^2 = 1.$$

The vertices will be given by rational functions of u, u_1, u_2

$$P_1 = (a u, b u_1), \quad P_2 = (p_{2x}, p_{2y})/q_2, \quad P_3 = (p_{3x}, p_{3y})/q_3$$

Expressions for P_1, P_2, P_3 appear in Appendix C as do equations $g_i = 0$, $i = 1, 2, 3$, polynomial in s_i, u, u_1, u_2 .

Step 2. *Express the locus X as a rational function on $u, u_1, u_2, s_1, s_2, s_3$.*

Convert $p : q : r$ to Cartesians $X = (x, y)$ via Equation (1). From Lemma 5, it follows that (x, y) is rational on $u, u_1, u_2, s_1, s_2, s_3$.

$$x = \mathcal{Q}/\mathcal{R}, \quad y = \mathcal{S}/\mathcal{T}$$

To obtain the polynomials $\mathcal{Q}, \mathcal{R}, \mathcal{S}, \mathcal{T}$ on said variables $u, u_1, u_2, s_1, s_2, s_3$, one substitutes the p, q, r by the corresponding rational functions of s_1, s_2, s_3 that define a specific Triangle Center X . Other than that, the method proceeds identically.

Step 3. *Computing resultants.* Our problem is now cast in terms of the polynomial equations:

$$E_0 = \mathcal{Q} - x\mathcal{R} = 0, \quad F_0 = \mathcal{S} - y\mathcal{T} = 0$$

Firstly, compute the resultants, in chain fashion:

$$E_1 = \text{Res}(g_1, E_0, s_1) = 0$$

$$F_1 = \text{Res}(g_1, F_0, s_1) = 0$$

$$E_2 = \text{Res}(g_2, E_1, s_2) = 0$$

$$F_2 = \text{Res}(g_2, F_1, s_2) = 0$$

$$E_3 = \text{Res}(g_3, E_2, s_3) = 0$$

$$F_3 = \text{Res}(g_3, F_2, s_3) = 0$$

It follows that $E_3(x, u, u_1, u_2) = 0$ and $F_3(y, u, u_1, u_2) = 0$ are polynomial equations. In other words, s_1, s_2, s_3 have been eliminated.

Now eliminate the variables u_1 and u_2 by taking the following resultants:

$$E_4(x, u, u_2) = \text{Res}(E_3, u_1^2 + u^2 - 1, u_1) = 0$$

$$F_4(y, u, u_2) = \text{Res}(F_3, u_1^2 + u^2 - 1, u_1) = 0$$

$$E_5(x, u) = \text{Res}(E_4, u_2^2 + \rho_1 u^2 - 1, u_2) = 0$$

$$F_5(y, u) = \text{Res}(F_4, u_2^2 + \rho_1 u^2 - 1, u_2) = 0$$

This yields two polynomial equations $E_5(x, u) = 0$ and $F_5(y, u) = 0$.

Finally compute the resultant

$$\mathcal{L} = \text{Res}(E_5, F_5, u) = 0$$

that eliminates u and gives the implicit algebraic equation for the locus X .

Remark 2. *In practice, after obtaining a resultant, a human assists the CAS by factoring out spurious branches (when recognized), in order to get the final answer in more reduced form.*

When not rational in the sidelengths, except a few cases¹⁶, Triangle Centers in Kimberling's list have explicit Trilinears involving fractional powers and/or terms containing the triangle area. Those can be made implicit, i.e, given by zero sets of polynomials involving p, q, r, s_1, s_2, s_3 . The chain of resultants to be computed will be increased by three, in order to eliminate the variables p, q, r before (or after) s_1, s_2, s_3 .

¹⁶For instance Hofstadter points $X(359), X(360)$.

4.3.1. Supporting Lemmas.

Lemma 5. *Let $P_1 = (au, b\sqrt{1-u^2})$. The coordinates of P_2 and P_3 of the 3-periodic billiard orbit are rational functions in the variables u, u_1, u_2 , where $u_1 = \sqrt{1-u^2}$, $u_2 = \sqrt{1-\rho_1 u^2}$ and $\rho_1 = c^4(b^2 + \delta)^2/a^6$.*

Proof. Follows directly from the parametrization of the billiard orbit, Appendix C.2. In fact, $P_2 = (x_2(u), y_2(u)) = (p_{2x}/q_2, p_{2y}/q_2)$ and $P_3 = (x_3(u), y_3(u)) = (p_{3x}/q_3, p_{3y}/q_3)$, where p_{2x} , p_{2y} , p_{3x} and p_{3y} have degree 4 in (u, u_1, u_2) and q_2, q_3 are algebraic of degree 4 in u . Expressions for u_1, u_2 appear in Appendix C.1. \square

Lemma 6. *Let $P_1 = (au, b\sqrt{1-u^2})$. Let s_1, s_2 and s_3 the sides of the triangular orbit $P_1P_2P_3$. Then $g_1(u, s_1) = 0$, $g_2(s_2, u_2, u) = 0$ and $g_3(s_3, u_2, u) = 0$ for polynomial functions g_i .*

Proof. Using the parametrization of the 3-periodic billiard orbit it follows that $s_1^2 - |P_2 - P_3|^2 = 0$ is a rational equation in the variables u, s_1 . Simplifying, leads to $g_1(s_1, u) = 0$.

Analogously for s_2 and s_3 . In this case, the equations $s_2^2 - |P_1 - P_3|^2 = 0$ and $s_3^2 - |P_1 - P_2|^2 = 0$ have square roots $u_2 = \sqrt{1-\rho_1 u^2}$ and $u_1 = \sqrt{1-u^2}$ and are rational in the variables s_2, u_2, u_1, u and s_3, u_2, u_1, u respectively. It follows that the degrees of g_1, g_2 , and g_3 are 10. Simplifying, leads to $g_2(s_2, u_2, u_1, u) = 0$ and $g_3(s_3, u_2, u_1, u) = 0$. \square

4.4. Examples. Table 4 shows the Zariski closure obtained contained the elliptic locus of a few Triangle Centers. Notice one factor is always of the form $[(x/a_i)^2 + (y/b_i)^2 - 1]^3$, related to the triple cover described in Section 3.5. The expressions shown required some manual simplification during the symbolic calculations.

X_i	Name	Spurious Factors	Elliptic Factor	a_i	b_i
1	Incenter	very long expression	$[36(91 + 61\sqrt{61})x^2 + 324(139 + 19\sqrt{61})y^2 + 22761 - 3969\sqrt{61}]^6$	0.63504	0.29744
2	Barycenter	$(91500x^2 + 49922\sqrt{61} - 370993)^2$	$(100x^2 + 225y^2 + 52\sqrt{61} - 413)^3$	0.26205	0.1747
3	Circumcenter	$x(3600x^4 - 6380x^2 - 1539)(40x^2 + 5\sqrt{61} - 43)^2(-1104500y^2 + 591136\sqrt{61} - 4633685)^2(65880x^2 + 8527\sqrt{61} - 64649)^6$	$(5832x^2 + (2752 - 320\sqrt{61})y^2 + 5751 - 729\sqrt{61})^3$	0.099146	0.4763

TABLE 4. Method of Resultants applied to obtain the Zariski closure for a few sample Triangle Centers with elliptic loci, for the specific case of $a/b = 1.5$. Both spurious and an elliptic factor are present. The latter are raised to powers multiple of three suggesting a phenomenon related to the triple cover, Section 3.5. Also shown are semi-axes a_i, b_i implied by the elliptic factor. These have been checked to be in perfect agreement with the values predicted for those semi-axes in Appendix E.

5. CONCLUSION

A few interesting questions are posed to the reader.

- Are there conditions in the Trilinears of a Triangle Center so that its locus is an ellipse? Please refer to Table 3 for a few examples showing no apparent pattern.
- Can the degree of the locus of a Triangle Center or Derived Triangle vertex be predicted based on its Trilinears?
- Is there a Triangle Center such that its locus intersects a straight line more than 6 times?
- Certain Triangles Centers have non-convex loci (e.g., X_{67} at $a/b = 1.5$ [17]). What determines non-convexity?
- What determines the number of self-intersections of a given locus?
- In the spirit of [5, 21], how would one determine via complex analytic geometry, that X_6 is a quartic?
- What is the non-elliptic locus described by the summits of equilaterals erected over each orbit side (used in the construction of the Outer Napoleon Triangle [28]). [18, pl#13]. What kind of curve is it?
- Within X_1 and X_{100} only X_i , $i = 13 \dots 18$ have irrational Trilinears. X_j , $j = 359, 360, 364, 365, 367$ are irrational and have loci which numerically are non-elliptic. Can any irrational Center produce an ellipse?

5.1. Videos and Media. The reader is encouraged to browse our companion paper [20] where intriguing locus phenomena are investigated. Additionally, loci can be explore interactively with our [applet](#) [16].

Videos mentioned herein are on a [playlist](#) [18], with links provided on Table 5.

PL#	Title	Section
01	Locus of X_1 is an Ellipse	1
02	Locus of Intouchpoints is non-elliptic	1, 2
03	X_9 stationary at EB center	1
04	Stationary Excentral Cosine Circle	1
05	Loci for $X_1 \dots X_5$ are ellipses	2
06	Elliptic locus of Excenters similar to rotated X_1	2
07	Loci of X_{11} , X_{100} and Extouchpoints are the EB	2
08	Family of Derived Triangles	3
09	Loci of Vertices of Derived Triangles	2,3
10	Peter Moses' 29 Billiard Points	3
11	Locus of Convex Comb.: X_1 -Intouch and X_2 -Midpoint	3.5
12	Locus of Convex Comb.: X_3 -Midpoint and X_4 -Altfoot	3.5
13	Oval Locus of the Outer Napoleon Summits	5

TABLE 5. Videos mentioned in the paper. Column “PL#” indicates the entry within the playlist [18].

ACKNOWLEDGMENTS

We warmly thank Clark Kimberling, Peter Moses, Sergei Tabachnikov, Richard Schwartz, Arseniy Akopyan, Olga Romaskevich, Ethan Cotterill, for their input during this research.

The first author is fellow of CNPq and coordinator of Project PRONEX/CNPq/ FAPEG 2017 10 26 7000 508.

REFERENCES

- [1] Akopyan, A., Schwartz, R., Tabachnikov, S.: Billiards in ellipses revisited (2020). URL <https://arxiv.org/abs/2001.02934>. ArXiv
- [2] Bialy, M., Tabachnikov, S.: Dan Reznik’s identities and more (2020). URL <https://arxiv.org/abs/2001.08469>. ArXiv
- [3] Cox, D., Little, J., O’Shea, D.: Using Algebraic Geometry. Springer (2005)
- [4] Dragović, V., Radnović, M.: Poncelet Porisms and Beyond: Integrable Billiards, Hyperelliptic Jacobians and Pencils of Quadrics. Frontiers in Mathematics. Springer, Basel (2011). URL <https://books.google.com.br/books?id=QcOmDAEACAAJ>
- [5] Fierobe, C.: On the circumcenters of triangular orbits in elliptic billiard (2018). URL <https://arxiv.org/pdf/1807.11903.pdf>. Submitted
- [6] Fitzgibbon, A., Pilu, M., Fisher, R.: Direct least square fitting of ellipses. Pattern Analysis and Machine Intelligence **21**(5) (1999)
- [7] Garcia, R.: Elliptic billiards and ellipses associated to the 3-periodic orbits. American Mathematical Monthly **126**(06), 491–504 (2019). URL <https://doi.org/10.1080/00029890.2019.1593087>
- [8] Griffiths, P., Harris, J.: On Cayley’s explicit solution to Poncelet’s porism. Enseign. Math. (2) **24**(1-2), 31–40 (1978)
- [9] Grozdev, S., Dekov, D.: The computer program “Discoverer” as a tool of mathematical investigation. International Journal of Computer Discovered Mathematics (IJCDM) (2014). URL <http://www.ddekov.eu/j/2014/JCGM201405.pdf>
- [10] Kaloshin, V., Sorrentino, A.: On the integrability of Birkhoff billiards. Phil. Trans. R. Soc. A(376) (2018). DOI <https://doi.org/10.1098/rsta.2017.0419>
- [11] Kimberling, C.: Triangle centers as functions. Rocky Mountain J. Math. **23**(4), 1269–1286 (1993). DOI 10.1216/rmjm/1181072493. URL <https://doi.org/10.1216/rmjm/1181072493>
- [12] Kimberling, C.: Encyclopedia of triangle centers (2019). URL <https://faculty.evansville.edu/ck6/encyclopedia/ETC.html>
- [13] Lang, S.: Algebra, *Graduate Texts in Mathematics*, vol. 211, third edn. Springer-Verlag, New York (2002). DOI 10.1007/978-1-4613-0041-0. URL <https://doi.org/10.1007/978-1-4613-0041-0>
- [14] Levi, M., Tabachnikov, S.: The Poncelet grid and billiards in ellipses. The American Mathematical Monthly **114**(10), 895–908 (2007). DOI 10.1080/00029890.2007.11920482. URL <https://doi.org/10.1080/00029890.2007.11920482>
- [15] Moore, R., Kearfott, R.B., Cloud, M.J.: Introduction to Interval Analysis. SIAM (2009)
- [16] Reznik, D.: Applet showing the locus of several triangular centers (2019). URL <https://editor.p5js.org/dreznik/full/i1Lin7lt7>
- [17] Reznik, D.: Triangular orbits in elliptic billiards: Loci of points X(1) X(100) (2019). URL https://dan-reznik.github.io/Elliptical-Billiards-Triangular-Orbits/loci_6tri.html
- [18] Reznik, D.: Playlist for “Loci of Triangular Orbits in an Elliptic Billiard: Elliptic? Algebraic?” (2020). URL <https://bit.ly/2RE0igc>

- [19] Reznik, D., Garcia, R., Koiller, J.: Can the elliptic billiard still surprise us? *Mathematical Intelligencer* (2019). DOI 10.1007/s00283-019-09951-2. URL <https://arxiv.org/pdf/1911.01515.pdf>
- [20] Reznik, D., Garcia, R., Koiller, J.: Intriguing loci of triangular orbits in elliptic billiards (2020). In preparation
- [21] Romaskevich, O.: On the incenters of triangular orbits on elliptic billiards. *Enseign. Math.* **60**(3-4), 247–255 (2014). DOI 10.4171/LEM/60-3/4-2. URL <https://arxiv.org/pdf/1304.7588.pdf>
- [22] Rozikov, U.A.: *An Introduction To Mathematical Billiards*. World Scientific Publishing Company (2018)
- [23] Schenck, H.: *Computational Algebraic Geometry*, London Mathematical Society Student Text, vol. 58. Cambridge University Press (2003)
- [24] Snyder, J.M.: Interval analysis for computer graphics. *Computer Graphics* **26**(2), 121–129 (1992)
- [25] Sturmfels, B.: Introduction to resultants, in *Applications of Computational Algebraic Geometry*, vol. 53, pp. 25–40. American Mathematical Society (1997). *Proceedings of Symposia in Applied Mathematics*
- [26] Tabachnikov, S.: *Geometry and Billiards*, *Student Mathematical Library*, vol. 30. American Mathematical Society, Providence, RI (2005). DOI 10.1090/stml/030. URL <http://www.personal.psu.edu/sot2/books/billiardsgeometry.pdf>. Mathematics Advanced Study Semesters, University Park, PA
- [27] Tabachnikov, S.: Projective configuration theorems: old wine into new wineskins. In: S. Dani, A. Papadopoulos (eds.) *Geometry in History*, pp. 401–434. Springer Verlag (2019). URL <https://arxiv.org/pdf/1607.04758.pdf>
- [28] Weisstein, E.: Mathworld (2019). URL <http://mathworld.wolfram.com>

APPENDIX A. REVIEW: ELLIPTIC BILLIARDS

An Elliptic Billiard (EB) is a particle moving with constant velocity in the interior of an ellipse, undergoing elastic collisions against its boundary [22, 26], Figure 11. For any boundary location, a given exit angle (e.g., measured from the normal) may give rise to either a quasi-periodic (never closes) or N -periodic trajectory [26], where N is the number of bounces before the particle returns to its starting location.

The EB is the only known *integrable* Billiard in the plane [10]. It satisfies two important integrals of motion: (i) Energy, since particle velocity has constant modulus and bounces are elastic, and (ii) Joachimsthal’s, implying that all trajectory segments are tangent to a confocal Caustic [26]. The EB is a special case of *Poncelet’s Porism* [4]: if one N -periodic trajectory can be found departing from some boundary point, any other such point will initiate an N -periodic, i.e., a 1d *family* of such orbits will exist. A striking consequence of Integrability is that for a given N , all N -periodics have the same perimeter [26].

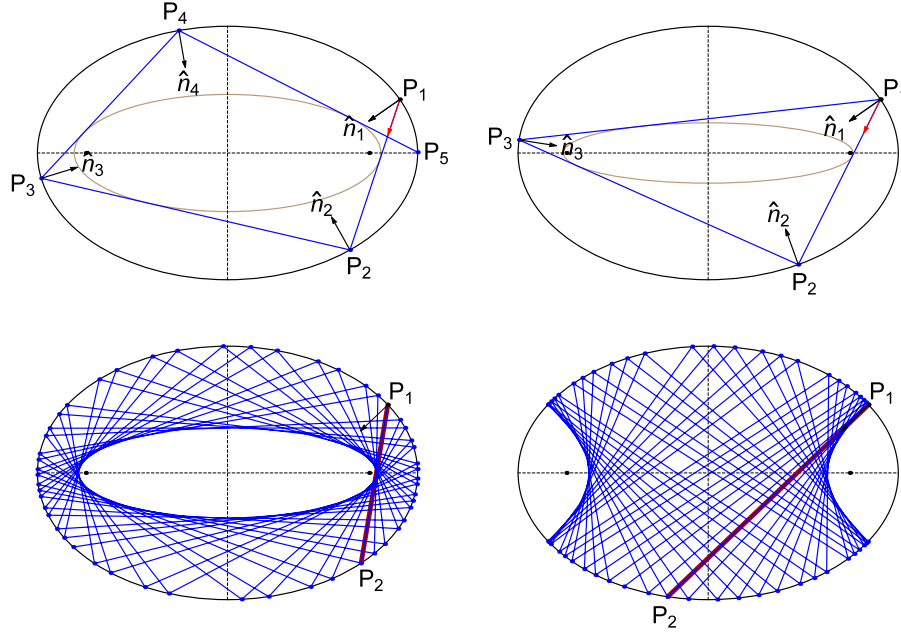


FIGURE 11. Trajectory regimes in an Elliptic Billiard, taken from [19]. **Top left**: first four segments of a trajectory departing at P_1 and toward P_2 , bouncing at $P_i, i = 2, 3, 4$. At each bounce the normal \hat{n}_i bisects incoming and outgoing segments. Joachimsthal's integral [26] means all segments are tangent to a confocal *Caustic* (brown). **Top right**: a 3-periodic trajectory. All 3-periodics in this Billiard will be tangent to a special confocal Caustic (brown). **Bottom**: first 50 segments of a non-periodic trajectory starting at P_1 and directed toward P_2 . Segments are tangent to a confocal ellipse (left) or hyperbola (right). The former (resp. latter) occurs if P_1P_2 passes outside (resp. between) the EB's foci (black dots).

APPENDIX B. TRIANGLE CENTERS

A point on the plane of a triangle $T = P_1P_2P_3$ can be defined by a triple $p : q : r$ of signed distances to each side¹⁷, see Figure 2. This local coordinate system renders the point invariant under similarity transformations (rigid+dilation+reflection) of T .

A *Triangle Center* is such a triple obtained by applying a *Triangle Center Function* h thrice to the sidelengths s_1, s_2, s_3 cyclically [11]:

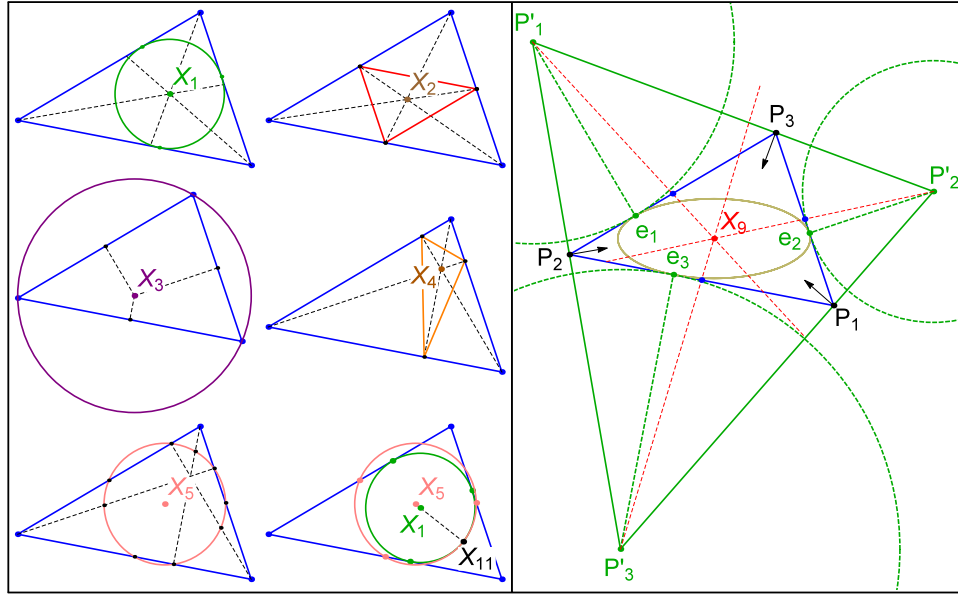
$$(5) \quad p : q : r \iff h(s_1, s_2, s_3) : h(s_2, s_3, s_1) : h(s_3, s_1, s_2)$$

h must (i) be *bi-symmetric*, i.e., $h(s_1, s_2, s_3) = h(s_1, s_3, s_2)$, and (ii) homogeneous, $h(ts_1, ts_2, ts_3) = t^n h(s_1, s_2, s_3)$ for some n [11].

Triangle Center Functions for a few Triangle Centers catalogued in [28] appears in Table 3. Trilinears can be converted to Cartesians using (1).

B.1. Constructions for Basic Triangle Centers. Constructions for a few basic Triangle Centers are shown in Figure 12.

¹⁷The Barycentrics of $p : q : r$ are $p s_1 : q s_2 : r s_3$ [28].

FIGURE 12. Constructions for Triangle Centers X_i , $i = 1, 2, 3, 4, 5, 9, 11$, taken from [19].

- The Incenter X_1 is the intersection of angular bisectors, and center of the Incircle (green), a circle tangent to the sides at three *Intouch-points* (green dots), its radius is the *Inradius* r .
- The Barycenter X_2 is where lines drawn from the vertices to opposite sides' midpoints meet. Side midpoints define the *Medial Triangle* (red).
- The Circumcenter X_3 is the intersection of perpendicular bisectors, the center of the *Circumcircle* (purple) whose radius is the *Circum-radius* R .
- The Orthocenter X_4 is where altitudes concur. Their feet define the *Orthic Triangle* (orange).
- X_5 is the center of the 9-Point (or Euler) Circle (pink): it passes through each side's midpoint, altitude feet, and Euler Points [28].
- The Feuerbach Point X_{11} is the single point of contact between the Incircle and the 9-Point Circle.
- Given a reference triangle $P_1P_2P_3$ (blue), the *Excenters* $P'_1P'_2P'_3$ are pairwise intersections of lines through the P_i and perpendicular to the bisectors. This triad defines the *Excentral Triangle* (green).
- The *Excircles* (dashed green) are centered on the Excenters and are touch each side at an *Extouch Point* $e_i, i = 1, 2, 3$.
- Lines drawn from each Excenter through sides' midpoints (dashed red) concur at the *Mittenpunkt* X_9 .
- Also shown (brown) is the triangle's *Mandart Inellipse*, internally tangent to each side at the e_i , and centered on X_9 . This is identical to the $N = 3$ Caustic.

B.2. Derived Triangles. A *Derived Triangle* T' is constructed from the vertices of a reference triangle T . A convenient representation is a 3×3 matrix, where each row, taken as Trilinears, is a vertex of T' . For example, the Excentral, Medial, and Intouch Triangles are given by [28]:

$$T'_{exc} = \begin{bmatrix} -1 & 1 & 1 \\ 1 & -1 & 1 \\ 1 & 1 & -1 \end{bmatrix}, \quad T'_{med} = \begin{bmatrix} 0 & s_2^{-1} & s_3^{-1} \\ s_1^{-1} & 0 & s_3^{-1} \\ s_1^{-1} & s_2^{-1} & 0 \end{bmatrix}$$

$$T'_{int} = \begin{bmatrix} 0 & \frac{s_1 s_3}{s_1 - s_2 + s_3} & \frac{s_1 s_2}{s_1 + s_2 - s_3} \\ \frac{s_2 s_3}{-s_1 + s_2 + s_3} & 0 & \frac{s_1 s_2}{s_1 + s_2 - s_3} \\ \frac{s_2 s_3}{-s_1 + s_2 + s_3} & \frac{s_1 s_3}{s_1 - s_2 + s_3} & 0 \end{bmatrix}$$

A few Derived Triangles are shown in Figure 13, showing a property similar to Lemma 2, Appendix D, namely, when the 3-periodic is an isosceles, one vertex of the Derived Triangle lies on the orbit's axis of symmetry.

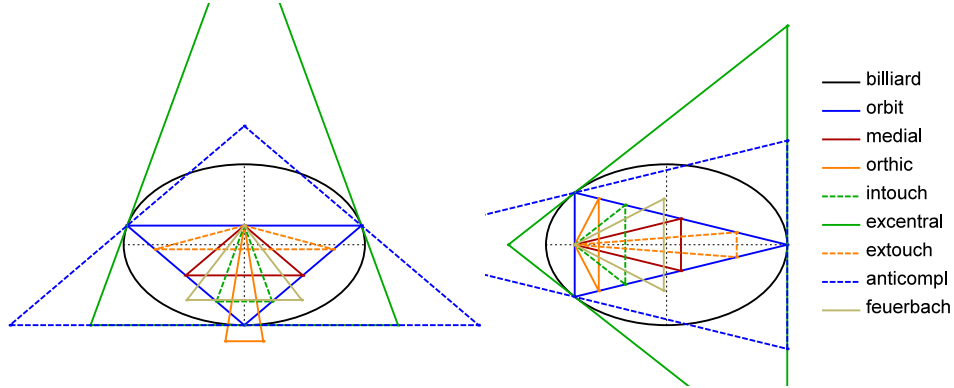


FIGURE 13. When the orbit is an isosceles triangle (solid blue), any Derived Triangle will contain one vertex on the axis of symmetry of the orbit. **Video:** [18, pl#08]

APPENDIX C. EXPRESSIONS USED IN SECTION 4.3

Let the boundary of the Billiard satisfy Equation (2). Assume, without loss of generality, that $a \geq b$. Here we provide expressions used in Section 4. Let P_1, P_2, P_3 be an orbit's vertices.

C.1. Exit Angle Required for 3-Periodicity. Consider a starting point $P_1 = (x_1, y_1)$ on a Billiard with semi-axes a, b . The cosine of the exit angle α (measured with respect to the normal at P_1 ¹⁸) required for the trajectory to close after 3 bounces is given by [7]:

¹⁸i.e., $\alpha = \theta_1/2$.

$$\begin{aligned}\cos^2 \alpha &= \frac{d_1^2 \delta_1^2}{d_2} = k_1, \\ \sin \alpha \cos \alpha &= \frac{\delta_1 d_1^2}{d_2} \sqrt{d_2 - d_1^4 \delta_1^2} = k_2\end{aligned}$$

with:

$$\begin{aligned}c^2 &= a^2 - b^2, \quad d_1 = (a b/c)^2, \quad d_2 = b^4 x_1^2 + a^4 y_1^2 \\ \delta &= \sqrt{a^4 + b^4 - a^2 b^2}, \quad \delta_1 = \sqrt{2\delta - a^2 - b^2}\end{aligned}$$

C.2. Orbit Vertices. Given a starting vertex $P_1 = (x_1, y_1)$ on the EB, $P_2 = (p_{2x}, p_{2y})/q_2$, and $P_3 = (p_{3x}, p_{3y})/q_3$ where [7]:

$$\begin{aligned}p_{2x} &= -b^4 ((a^2 + b^2) k_1 - a^2) x_1^3 - 2a^4 b^2 k_2 x_1^2 y_1 \\ &\quad + a^4 ((a^2 - 3b^2) k_1 + b^2) x_1 y_1^2 - 2a^6 k_2 y_1^3 \\ p_{2y} &= 2b^6 k_2 x_1^3 + b^4 ((b^2 - 3a^2) k_1 + a^2) x_1^2 y_1 \\ &\quad + 2a^2 b^4 k_2 x_1 y_1^2 - a^4 ((a^2 + b^2) k_1 - b^2) y_1^3 \\ q_2 &= b^4 (a^2 - c^2 k_1) x_1^2 + a^4 (b^2 + c^2 k_1) y_1^2 - 2a^2 b^2 c^2 k_2 x_1 y_1 \\ p_{3x} &= b^4 (a^2 - (b^2 + a^2)) k_1 x_1^3 + 2a^4 b^2 k_2 x_1^2 y_1 \\ &\quad + a^4 (k_1 (a^2 - 3b^2) + b^2) x_1 y_1^2 + 2a^6 k_2 y_1^3 \\ p_{3y} &= -2b^6 k_2 x_1^3 + b^4 (a^2 + (b^2 - 3a^2) k_1) x_1^2 y_1 \\ &\quad - 2a^2 b^4 k_2 x_1 y_1^2 + a^4 (b^2 - (b^2 + a^2) k_1) y_1^3, \\ q_3 &= b^4 (a^2 - c^2 k_1) x_1^2 + a^4 (b^2 + c^2 k_1) y_1^2 + 2a^2 b^2 c^2 k_2 x_1 y_1.\end{aligned}$$

C.3. Polynomials Satisfied by the Sidelengths. Let sidelengths $s_1 = |P_3 - P_2|$, $s_2 = |P_1 - P_3|$, $s_3 = |P_2 - P_1|$. The following are polynomial expressions on s_i and u, u_1, u_2 :

$$\begin{aligned}
 g_1 &= -h_1 s_1^2 + h_0 \\
 g_2 &= -h_1 s_2^2 - h_2 u_1 u_2 + h_3 \\
 g_3 &= -h_1 s_3^2 + h_2 u_1 u_2 + h_3 \\
 h_0 &= 12c^{12}(a^2 + b^2 + 2\delta)u^8 + 24c^{10}(a^2b^2 + 2b^4 - 2\delta c^2u^6 \\
 &\quad - 4c^4[10a^{10} - 12a^8b^2 + 11a^6b^4 - 7a^4b^6 + 24a^2b^8 - 8b^{10} \\
 &\quad - (2(4a^4 - 2a^2b^2 + b^4))(a^4 - 2a^2b^2 + 4b^4)\delta]u^4 \\
 &\quad + 8a^6c^2[4a^6 - 7a^4b^2 + 11a^2b^4 - 2b^6 - (2(a^2 + ab + b^2))(a^2 - ab + b^2)\delta]u^2 \\
 &\quad + 4a^{12}\delta_1^2 \\
 h_1 &= c^2(3c^4u^4 - 2c^2(a^2 - 2b^2u^2 - a^4))^2 \\
 h_2 &= -2a(b^2 - \delta)\delta_1u((3c^6\delta + (6(a^2 + b^2))c^6)u^6 + ((3(a^2 + 4b^2))c^4\delta \\
 &\quad - (3(2a^4 - a^2b^2 - 4b^4))c^4)u^4 + ((b_2 - a^2)(7a^4 - 8b^4)\delta \\
 &\quad + 2c^2(a^2 - 2b^2)(a^4 - 2b^4))u^2 + a^4(a^2 - 4b^2)\delta - a^4(2a^4 - 3a^2b^2 + 4b^4)) \\
 h_3 &= c^6(9c^6u^{10} + 1)((18(a^4 + b^4))\delta - (3(7a^6 - 16a^4b^2 + 29a^2b^4 - 8b^6))u^8 \\
 &\quad + 2c^2[(13a^8 - 12a^6b^2 + 49a^4b^4 - 54a^2b^6 + 16b^8) \\
 &\quad - 2(10a^6 - 7a^4b^2 + 11a^2b^4 - 8b^6)\delta]u^6 \\
 &\quad + ((28a^4\delta^2 - 40a^2b^6 + 16b^8)\delta - 26a^{10} + 12a^8b^2 + 42a^4b^6 - 48a^2b^8 + 16b^{10})u^4 \\
 &\quad + a(13a^6 - 9a^4b^2 - 8b^4c^2 - (4(2a^4 + a^2b^2 - 2b^4))\delta)^4u^2 + 2a^8(\delta - a^8c^2)
 \end{aligned}$$

APPENDIX D. PROOF OF LEMMAS USED IN SECTION 3

Lemma (4). *A parametric traversal of P_1 around the EB boundary is a triple cover of the locus of a Triangle Center X_i .*

Proof. Let $P_1(t) = (a \cos t, b \sin t)$. Let t^* (resp. t^{**}) be the value of t for which the 3-periodic orbit is an isosceles with a horizontal (resp. vertical) axis of symmetry, Figure 14, $t^* > t^{**}$. For such cases one can easily derive¹⁹:

$$\tan t^* = \frac{b\sqrt{2\delta - a^2 + 2b^2}}{a^2}, \quad \tan t^{**} = \frac{\sqrt{2\delta - 2a^2 + b^2}}{\sqrt{3}a}$$

with $\delta = \sqrt{a^4 - a^2b^2 + b^4}$ as above. Referring to Figure 14:

Affirmation 1. *A continuous counterclockwise motion of $P_1(t)$ along the intervals $[-t^*, -t^{**})$, $[-t^{**}, 0)$, $[0, t^{**})$, and $[t^{**}, t^*)$ will each cause X_i to execute a quarter turn along its locus, i.e., with t varying from $-t^*$ to t^* , X_i will execute one complete revolution on its locus²⁰.*

¹⁹It turns out $\sin t^* = Jb$ and $\cos t^{**} = Ja$, where J is the $N = 3$ Joachmishal's constant [26].

²⁰The direction of this revolution depends on X_i and its not always monotonic. The observation is valid for elliptic or non-elliptic loci alike.

Affirmation 2. *A continuous counterclockwise motion of $P_1(t)$ in the $[t^*, \pi - t^*)$ (resp. $[\pi - t^*, \pi + t^*)$, and $[\pi + t^*, 2\pi - t^*)$), visits the same 3-periodics as when t sweeps $[-t^*, -t^{**})$ (resp. $[-t^*, t^*)$, and $[t^*, \pi - t^*)$).*

Therefore, a complete turn of $P_1(t)$ around the EB visits the 3-periodic family thrice, i.e., X_i will wind thrice over its locus. \square

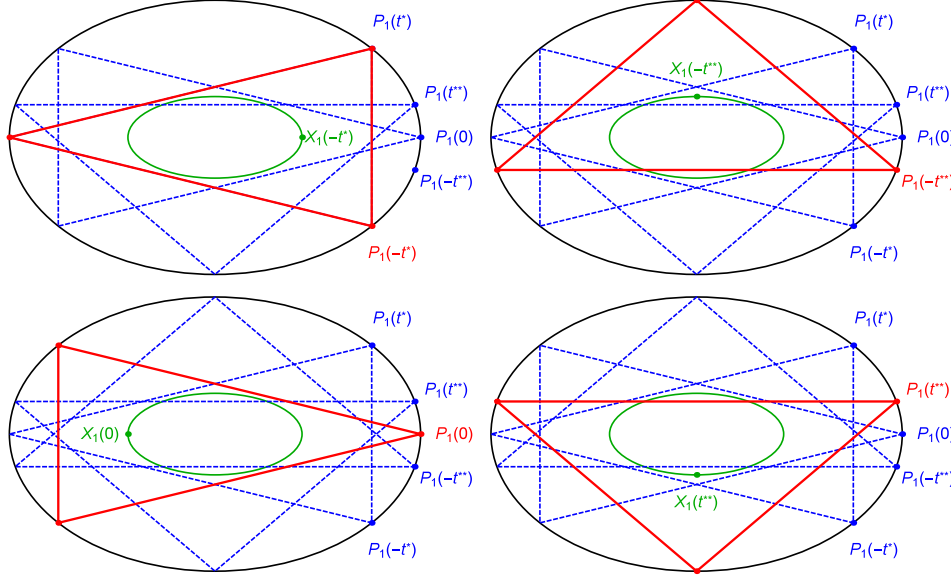


FIGURE 14. Counterclockwise motion of $P_1(t)$, for $t = [-t^*, t^*)$ can be divided in four segments delimited by $t = (-t^*, -t^{**}, 0, t^{**}, t^*)$. Orbit positions for the first four are shown (red polygons) in the top-left, top-right, bot-left, and bot-right pictures. At $P_1(\pm t^*)$ (resp. $P_1(\pm t^{**})$) the orbit is an isosceles triangle with a horizontal (resp. vertical) axis of symmetry. Observations 1,2 assert that a counterclockwise motion of $P_1(t)$ along each of the four intervals causes a Triangle Center X_i to execute a quarter turn along its locus (elliptic or not), and that a complete revolution of $P_1(t)$ around the EB causes X_i to wind thrice on its locus. For illustration, the locus of $X_1(t)$ is shown (green) at each of the four interval endpoints.

Below we provide proofs of Lemmas 2, 3 and 4.

Lemma (2). *Any Triangle Center X_i of an isosceles triangle is on the axis of symmetry of said triangle.*

Proof. Consider a sideways isosceles triangle with vertices $P_1 = (x_1, 0)$, $P_2 = (-x_2, y_2)$ and $P_3 = (-x_2, -y_2)$, i.e., its axis of symmetry is the x axis. Let X_i have Trilinears $p : q : r = h(s_1, s_2, s_3) : h(s_2, s_3, s_1) : h(s_3, s_1, s_2)$. Its Cartesians are given by Equation (1). As $s_2 = s_3$ and h is symmetric on its last two variables $h(s_1, s_2, s_3) = h(s_1, s_3, s_2)$ it follows from equation (1) that $y_i = 0$. \square

Lemma (3). *If the locus of Triangle Center X_i is elliptic, said ellipse must be concentric and axis-aligned with the EB.*

Proof. This follows from Lemma 1. \square

Lemma (4). *If the locus of X_i is an ellipse, when $P_1(t)$ is at either EB vertex, its non-zero coordinate is equal to the corresponding locus semi-axis length.*

Proof. The family of 3-periodic orbits contains four isosceles triangles, Figure 5. Parametrize $P_1(t) = (a \cos t, b \sin t)$. It follows from Lemma 3 that $X_i(0) = (\pm a_i, 0)$, $X_i(\pi/2) = (0, \pm b_i)$, $X_i(\pi) = (\mp a_i, 0)$ and $X_i(3\pi/2) = (0, \mp b_i)$, for some a_i, b_i . This ends the proof. \square

APPENDIX E. SEMIAXES OF THE 29 ELLIPTIC LOCI

Table 1 lists the 29 of the first 100 Kimberling centers whose loci ellipses concentric and axis-aligned with the Billiard. Below we provide explicit expressions for the semi-axes a_i, b_i of said loci, i.e., let the locus of center X_i be described as:

$$\frac{x^2}{a_i^2} + \frac{y^2}{b_i^2} = 1$$

As above, $\delta = \sqrt{a^4 - a^2b^2 + b^4}$. Also, the following explicit expressions were given for the axes of the $N = 3$ Caustic [7]:

$$a_c = \frac{a(\delta - b^2)}{c^2}, \quad b_c = \frac{b(a^2 - \delta)}{c^2}.$$

Two concentric, axis-aligned ellipses can generate a 3-periodic Poncelet family if and only if $a/a_c + b/b_c = 1$ [8], which holds above.

E.1. X_1 and Excenters.

$$a_1 = \frac{\delta - b^2}{a}, \quad b_1 = \frac{a^2 - \delta}{b}$$

The locus of the Excenters is an ellipse with axes:

$$a_e = \frac{b^2 + \delta}{a}, \quad b_e = \frac{a^2 + \delta}{b}$$

Notice it is similar to the X_1 locus, i.e., $a_1/b_1 = b_e/a_e$.

E.2. X_2 (similar to Billiard).

$$(a_2, b_2) = k_2 (a, b), \text{ where } k_2 = \frac{2\delta - a^2 - b^2}{3c^2}$$

E.3. X_3 (similar to rotated Caustic).

$$a_3 = \frac{a^2 - \delta}{2a}, \quad b_3 = \frac{\delta - b^2}{2b}$$

Additionally, when $a/b = \frac{\sqrt{2\sqrt{33}+2}}{2} \simeq 1.836$, $b_3 = b$, i.e., the top and bottom vertices of the locus of X_3 coincide with the Billiard's.

E.4. X_4 (similar to rotated Billiard).

$$(a_4, b_4) = \left(\frac{k_4}{a}, \frac{k_4}{b} \right), \quad k_4 = \frac{(a^2 + b^2)\delta - 2a^2b^2}{c^2}$$

Additionally:

- When $a/b = a_4 = \sqrt{2\sqrt{2}-1} \simeq 1.352$, $b_4 = b$, i.e., the top and bottom vertices of the locus of X_4 coincide with the Billiard's.
- Let a_4^* be the positive root of $x^6 + x^4 - 4x^3 - x^2 - 1 = 0$, i.e., $a_4^* \simeq 1.51$. When $a/b = a_4^*$, $a_4 = b$ and $b_4 = a$, i.e., the locus of X_4 is identical to a rotated copy of Billiard.

E.5. X_5 .

$$a_5 = \frac{-w'_5(a, b) + w''_5(a, b)\delta}{w_5(a, b)}, \quad b_5 = \frac{w'_5(b, a) - w''_5(b, a)\delta}{w_5(b, a)}$$

$$w'_5(u, v) = u^2(u^2 + 3v^2), \quad w''_5(u, v) = 3u^2 + v^2, \quad w_5(u, v) = 4u(u^2 - v^2).$$

E.6. X_7 (similar to Billiard).

$$(a_7, b_7) = k_7(a, b), \quad k_7 = \frac{2\delta - a^2 - b^2}{c^2}$$

E.7. X_8 .

$$a_8 = \frac{(b^2 - \delta)^2}{ac^2}, \quad b_8 = \frac{(a^2 - \delta)^2}{bc^2}$$

E.8. X_{10} (similar to rotated Billiard).

$$(a_{10}, b_{10}) = \left(\frac{k_{10}}{a}, \frac{k_{10}}{b} \right), \quad k_{10} = \frac{(a^2 + b^2)\delta - a^4 - b^4}{2c^2}$$

E.9. X_{11} (identical to Caustic).

$$a_{11} = a_c, \quad b_{11} = b_c$$

E.10. X_{12} .

$$a_{12} = \frac{-w'_{12}(a, b) + w''_{12}(a, b)\delta}{w_{12}(a, b)}, \quad b_{12} = \frac{w'_{12}(b, a) - w''_{12}(b, a)\delta}{w_{12}(b, a)}$$

$$w'_{12}(u, v) = v^2(15u^6 + 12v^2u^4 + 3u^2v^4 + 2v^6)$$

$$w''_{12}(u, v) = 7u^6 + 12v^2u^4 + 11u^2v^4 + 2v^6$$

$$w_{12}(u, v) = u(7u^6 + 11v^2u^4 - 11u^2v^4 - 7v^6).$$

E.11. X_{20} .

$$a_{20} = \frac{a^2(3b^2 - a^2) - 2b^2\delta}{ac^2}, \quad b_{20} = \frac{b^2(b^2 - 3a^2) + 2a^2\delta}{bc^2}$$

E.12. X_{21} .

$$a_{21} = \frac{-w'_{21}(a, b) + w''_{21}(a, b)\delta}{w_{21}(a, b)}, \quad b_{21} = \frac{w'_{21}(b, a) - w''_{21}(b, a)\delta}{w_{21}(b, a)}$$

$$w'_{21}(u, v) = u^4 + u^2 v^2 + v^4, \quad w''_{21}(u, v) = 2(u^2 + v^2), \quad w_{21}(u, v) = u(3u^2 + 5v^2)$$

E.13. X_{35} .

$$a_{35} = \frac{-w'_{35}(a, b) + w''_{35}(a, b)\delta}{w_{35}(a, b)}, \quad b_{35} = \frac{-w'_{35}(b, a) + w''_{35}(b, a)\delta}{w_{35}(b, a)}$$

$$w'_{35}(u, v) = v^2(11u^4 + 4u^2 v^2 + v^4), \quad w''_{35}(u, v) = (7u^2 + v^2)(u^2 + v^2)$$

$$w_{35}(u, v) = u(7u^4 + 18u^2 v^2 + 7v^4)$$

E.14. X_{36} .

$$a_{36} = \frac{w'_{36}(a, b) + w''_{36}(a, b)\delta}{w_{36}(a, b)}, \quad b_{36} = \frac{-w'_{36}(b, a) - w''_{36}(b, a)\delta}{w_{36}(b, a)}$$

$$w'_{36}(u, v) = v^2(u^2 + v^2), \quad w''_{36}(u, v) = 3u^2 - v^2, \quad w_{36}(u, v) = 3u(u^2 - v^2)$$

E.15. X_{40} (similar to rotated Billiard).

$$a_{40} = \frac{c^2}{a}, \quad b_{40} = \frac{c^2}{b}$$

Additionally:

- When $a/b = \sqrt{2}$, $b_{40} = b$, i.e., the top and bottom vertices of the X_{40} locus coincides with the Billiard's.
- When $a/b = (1 + \sqrt{5})/2 = \phi \simeq 1.618$, $b_{40} = a$ and $a_{40} = b$, i.e., the X_{40} locus is identical to a rotated copy of Billiard.

E.16. X_{46} .

$$a_{46} = \frac{w'_{46}(a, b) + w''_{46}(a, b)\delta}{w_{46}(a, b)}, \quad b_{46} = \frac{-w'_{46}(b, a) - w''_{46}(b, a)\delta}{w_{46}(b, a)}$$

$$w'_{46}(u, v) = v^2(3u^2 - v^2)(u^2 - v^2), \quad w''_{46}(u, v) = (5u^2 + v^2)(u^2 - v^2)$$

$$w_{46}(u, v) = v(5u^4 - 6u^2 v^2 + 5v^4)$$

E.17. X_{55} (similar to Caustic).

$$a_{55} = \frac{a(\delta - b^2)}{a^2 + b^2}, \quad b_{55} = \frac{b(a^2 - \delta)}{a^2 + b^2}$$

E.18. X_{56} .

$$a_{56} = \frac{-w'_{56}(a, b) + w''_{56}(a, b)\delta}{w_{56}(a, b)}, \quad b_{56} = \frac{w'_{56}(b, a) - w''_{56}(b, a)\delta}{w_{56}(b, a)}$$

$$\begin{aligned} w'_{56}(u, v) &= v^2(u^4 - u^2v^2 + 2v^4), \quad w''_{56}(u, v) = 5u^4 - 5u^2v^2 + 2v^4 \\ w_{56}(u, v) &= u(5u^4 - 6u^2v^2 + 5v^4) \end{aligned}$$

E.19. X_{57} (similar to Billiard).

$$(a_{57}, b_{57}) = k_{57}(a, b), \quad k_{57} = \frac{c^2}{\delta}$$

E.20. X_{63} (similar to Billiard).

$$(a_{63}, b_{63}) = k_{63}(a, b), \quad k_{63} = \frac{c^2}{a^2 + b^2}$$

E.21. X_{65} .

$$a_{65} = \frac{w'_{65}(a, b) + w''_{65}(a, b)\delta}{w_{65}(a, b)}, \quad b_{65} = \frac{-w'_{65}(b, a) - w''_{65}(b, a)\delta}{w_{65}(b, a)}$$

$$\begin{aligned} w'_{65}(u, v) &= u^4v^2 + u^2v^4 + 2v^6, \quad w''_{65}(u, v) = u^4 - 3u^2v^2 - 2v^4 \\ w_{65}(u, v) &= u(u^2 - v^2)^2 \end{aligned}$$

E.22. X_{72} .

$$a_{72} = \frac{w'_{72}(a, b) - w''_{72}(a, b)\delta}{w_{72}(a, b)}, \quad b_{72} = \frac{-w'_{72}(b, a) + w''_{72}(b, a)\delta}{w_{72}(b, a)}$$

$$w'_{72}(u, v) = u^6 + 2u^2v^4 + v^6, \quad w''_{72}(u, v) = (3u^2 + v^2)v^2, \quad w_{72}(u, v) = u(u^2 - v^2)^2$$

E.23. X_{78} .

$$a_{78} = \frac{w'_{78}(a, b) - w''_{78}(a, b)\delta}{w_{78}(a, b)}, \quad b_{78} = \frac{-w'_{78}(b, a) + w''_{78}(b, a)\delta}{w_{78}(b, a)}$$

$$\begin{aligned} w'_{78}(u, v) &= 5u^6 - 4u^4v^2 + u^2v^4 + 2v^6, \quad w''_{78}(u, v) = 2v^2(u^2 + v^2) \\ w_{78}(u, v) &= u(5u^4 - 6v^2u^2 + 5v^4) \end{aligned}$$

E.24. X_{79} .

$$a_{79} = \frac{-w'_{79}(a, b) + w''_{79}(a, b)\delta}{w_{79}(a, b)}, \quad b_{79} = \frac{w'_{79}(b, a) - w''_{79}(b, a)\delta}{w_{79}(b, a)}$$

$$\begin{aligned} w'_{79}(u, v) &= v^2(11u^4 + 4v^2u^2 + v^4), \quad w''_{79}(u, v) = (3u^4 + 12u^2v^2 + v^4) \\ w_{79}(u, v) &= u(u^2 - v^2)(3u^2 + 5v^2) \end{aligned}$$

E.25. X_{80} .

$$a_{80} = \frac{(\delta - b^2)(a^2 + b^2)}{ac^2}, \quad b_{80} = \frac{(a^2 - \delta)(a^2 + b^2)}{bc^2}$$

E.26. X_{84} (**similar to rotated Caustic**).

$$a_{84} = \frac{(b^2 + \delta)c^2}{a^3}, \quad b_{84} = \frac{(a^2 + \delta)c^2}{b^3}$$

E.27. X_{88} (**identical to Billiard**).

$$a_{88} = a, \quad b_{88} = b$$

E.28. X_{90} .

$$a_{90} = \frac{w'_{90}(a, b) + w''_{90}(a, b)\delta}{w_{90}(a, b)}, \quad b_{90} = \frac{w'_{90}(b, a) + w''_{90}(b, a)\delta}{w_{90}(b, a)}$$

$$w'_{90}(u, v) = v^2(3u^2 - v^2)(u^2 - v^2), \quad w''_{90}(u, v) = u^4 - v^4$$

$$w_{90}(u, v) = u(u^4 + 2u^2v^2 - 7v^4)$$

E.29. X_{100} (**identical to Billiard**).

$$a_{100} = a, \quad b_{100} = b$$

APPENDIX F. TABLE OF LEAST-SQUARES

Least-squares elliptic fit errors for the first 100 Kimberling Centers are tabulated in Table 6 in ascending order of error, see (3).

rank	X_i	\hat{a}	\hat{b}	$\sum err^2$
1	100	1.50	1.00	5.9×10^{-14}
2	80	1.65	0.77	8.1×10^{-14}
3	46	1.47	1.18	8.3×10^{-14}
4	36	2.57	2.34	$1. \times 10^{-13}$
5	88	1.50	1.00	$1. \times 10^{-13}$
6	56	1.05	0.74	1.1×10^{-13}
7	20	1.18	2.43	1.1×10^{-13}
8	72	0.75	0.35	1.1×10^{-13}
9	63	0.58	0.38	1.2×10^{-13}
10	40	0.83	1.25	1.3×10^{-13}
11	78	1.12	0.28	1.3×10^{-13}
12	57	0.96	0.64	1.4×10^{-13}
13	79	0.85	0.68	1.4×10^{-13}
14	4	0.98	1.48	1.4×10^{-13}
15	65	0.90	0.58	1.4×10^{-13}
16	7	0.79	0.52	1.5×10^{-13}
17	11	1.14	0.24	1.7×10^{-13}
18	5	0.44	0.50	1.7×10^{-13}
19	84	1.09	5.25	1.8×10^{-13}
20	12	0.55	0.38	1.8×10^{-13}
21	1	0.64	0.30	1.8×10^{-13}
22	2	0.26	0.17	2.3×10^{-13}
23	3	0.10	0.48	2.5×10^{-13}
24	55	0.44	0.09	2.9×10^{-13}
25	8	0.48	0.07	3.3×10^{-13}
26	10	0.08	0.11	3.6×10^{-13}
27	90	3.93	0.34	$4. \times 10^{-13}$
28	21	0.19	0.05	4.6×10^{-13}
29	35	0.33	0.03	4.8×10^{-13}

rank	X_i	$\sum err^2$
30	37	1.9×10^{-3}
31	6	6.2×10^{-3}
32	45	$8. \times 10^{-3}$
33	60	8.3×10^{-3}
34	86	1.3×10^{-2}
35	71	1.6×10^{-2}
36	41	1.8×10^{-2}
37	81	1.8×10^{-2}
38	58	3.3×10^{-2}
39	62	$4. \times 10^{-2}$
40	31	4.3×10^{-2}
41	89	4.4×10^{-2}
42	42	4.5×10^{-2}
43	17	5.6×10^{-2}
44	13	8.3×10^{-2}
45	83	$9. \times 10^{-2}$
46	48	1.1×10^{-1}
47	32	1.3×10^{-1}
48	61	1.3×10^{-1}
49	82	1.3×10^{-1}
50	43	1.5×10^{-1}
51	51	1.6×10^{-1}
52	85	1.6×10^{-1}
53	19	1.7×10^{-1}
54	27	1.9×10^{-1}
55	69	1.9×10^{-1}
56	47	2.5×10^{-1}
57	39	2.7×10^{-1}
58	38	2.8×10^{-1}
59	16	3.4×10^{-1}
60	52	5.3×10^{-1}
61	28	5.6×10^{-1}
62	25	7.5×10^{-1}
63	99	8.2×10^{-1}
64	14	8.3×10^{-1}
65	98	8.5×10^{-1}

rank	X_i	$\sum err^2$
66	44	1.7
67	22	1.7
68	34	1.7
69	75	1.9
70	54	2.1
71	53	2.2
72	29	2.4
73	15	2.5
74	33	2.6
75	24	2.6
76	74	3.2
77	97	3.3
78	67	4.
79	23	4.6
80	91	5.2
81	96	5.2
82	76	5.8
83	18	7.6
84	73	8.5
85	94	9.3
86	70	9.3
87	92	1.2×10^1
88	77	1.4×10^1
89	95	1.5×10^1
90	49	1.8×10^1
91	87	1.8×10^1
92	59	1.9×10^1
93	64	3.9×10^1
94	68	3.9×10^1
95	26	3.9×10^1
96	66	3.9×10^1
97	50	3.9×10^1
98	93	3.9×10^1
99	30	3.9×10^1
100	9	3.9×10^1

TABLE 6. Fit errors for first 100 Kimberling Centers ranked in ascending order of fit error, $a/b = 1.5$, $M = 1500$. **Left:** the 29 centers with elliptic loci, i.e., their fit errors are negligible. Columns \hat{a}, \hat{b} show the estimated semi-axes' lengths. Notice for X_{100} and X_{88} these are identical to a, b , since these points lie on the EB. **Middle:** non-elliptic centers whose fit error ranks 30–65. X_{37} has the least error in this table, 10 orders of magnitude higher than X_{35} , the last entry in the list of elliptic loci. **Right:** non-elliptic centers with errors ranking 66–100. Note X_9 displays the highest fit error of all centers, due to the fact that its locus is a point.

RONALDO GARCIA, INST. DE MATEMÁTICA E ESTATÍSTICA, UNIV. FEDERAL DE
GOIÁS, GOIÂNIA, GO, BRAZIL
E-mail address: `ragarcia@ufg.br`

DAN REZNIK, DATA SCIENCE CONSULTING, RIO DE JANEIRO, RJ, BRAZIL
E-mail address: `dan@dat-sci.com`

JAIR KOILLER, DEPT. DE MATEMÁTICA, UNIV. FEDERAL DE JUIZ DE FORA, JUIZ
DE FORA, MG, BRAZIL
E-mail address: `jairkoiller@gmail.com`